OPTIMAL DESIGN AND DYNAMIC ANALYSIS OF SNOWPLOW DECELERATOR
FOR AGRICULTURAL GREENHOUSES
/
农业大棚扫雪机减速器优化设计及动态特性分析

Ph.D. Xiangyang JIN [1), Ph.D. Eng. Hongling KANG [2) , B.S. Yiming SUN [1)
[1) School of Light Industry, Harbin University of Commerce, Harbin / China;
[2) Department of Mechanical Engineering, Keimyung College of Technology, Daegu /Republic of Korea
Tel:0451-84865182; E-mail: jinxiangyang@126.com

Abstract: A decelerator with high efficiency used in a snowplow for agricultural greenhouses was designed. Firstly, some decelerator types which can be used in snowplow were analyzed and a closed epi-cyclic gear, which has the effect of power-splitting, was used as the drivetrain of the deceleration system. A combination of the Ant Colony Algorithm and the Interior Point Penalty Function was adopted for the optimal design of the decelerator. Specifically, a structure that can be compensated has been designed to make sure the sealing security of the decelerator. To satisfy with the large torque of the decelerator, the finite element analysis (FEA) was performed for optimizing the key components of the decelerator. According to the FEA results, the decelerator was restructured to reach the optimum state. In addition, a virtual prototype model of the decelerator was established to make interference detection and motion simulation by using Pro/E software. As a result, the model was adjusted and checked by the above calculus, the interference was detected and removed. This paper offers the theoretical foundation to the mechanism designing and the simulation for the snowplow.

Keywords: Snowplow; Ant Colony Algorithm; Finite element analysis; Interference detection

INTRODUCTION

The heavy snow in winter is a serious disaster for the greenhouse. If not being promptly cleaned up, the deep snow will affect the growth of vegetable. Therefore, one of the urgent affairs currently is to find a way, which is more efficient, simply structured and with low cost [4], to clean the snow before covering the greenhouse with plastic films.

At present, there are four common snow removing methods including the artificial snow cleaning, the chemical deicing salt, the thermal deicing, and the mechanical deicing [3, 6, 7]. The artificial snow cleaning method has low efficiency and bad work environment. The chemical deicing salt pollutes the soil. The thermal deicing is an energy-consumed method with high cost. The mechanical deicing has been enjoyed in the widest application for having advantages of high sweeping efficiency and no pollution from chemicals. Snowplow for greenhouse has small size, required transmission power and transmission ratio is large, traditional bulky decelerator can not meet the requirement of snow cleaning equipment for greenhouse' use [1, 5, 9]. Therefore, this paper designed a new kind of decelerator for the greenhouse snowplow, which has the higher transmission power and smaller size.

The driving types of the snowplow decelerator were studied to select the best type. The improved Ant Colony

摘要：设计出一种高效农业大棚扫雪机用减速器。首先对能实现同轴减速的传动类型进行计算和分析,采用具有功率分流作用的封闭周转轮系作为减速系统的传动型式,将蚁群算法和内点惩罚函数法结合,对减速器进行优化设计。专门设计可补偿式结构来保证减速器的密封安全。为了满足减速器各元件在大扭矩作用下的强度要求,对减速器关键元件进行有限元分析,并根据分析结果对减速器结构进行调整以达到最优状态。利用 Pro/E 软件建立减速器的虚拟样机模型,进行干涉检测和运动仿真,根据仿真结果对减速器虚拟样机进行调整,去除干涉,并与理论计算进行验证。为农业大棚减速系统结构设计和计算机仿真提供理论依据。

关键词: 扫雪机; 蚁群算法; 有限元分析; 干涉检测

引言

冬季的暴风雪对农业大棚的危害巨大,如果不及时清理,积雪就会影响蔬菜的生长。因此,当务之急,是寻找一种高效、结构简单、低成本的大棚清雪方法[4],在覆膜之前能将大棚积雪清理干净。

目前,有四种常用的清雪方法,包括人工清雪法、化学溶解法、热熔法、机械清雪法[3,6,7]。人工清雪法效率低,工作环境恶劣。化学溶解法溶解冰雪虽然很有效,但有明显不足,就是污染土壤。热熔法比化学熔解法快,但能耗高,限制了其应用。机械清雪法效率高,无污染,应用日益广泛。大棚清雪设备体积小,要求传递的功率和传动比大,传统减速器体积大,不能满足大棚清雪设备的使用要求[1,5,9]。本文为大棚清雪设备设计了一种新型减速器,传动效率高,节省空间。

本文对扫雪机械的减速器的传动类型进行分析,选择最佳传动方式,对新型减速器的结构进行了创新设计,并进

Algorithm was adopted to build an optimum model. The result was compared with those of traditional optimization design methods. Next, the key components of the decelerator were checked and optimized by using the finite element analysis (FEA). The calculation to the important transmission part of the snowplow was checked. The 3D models of every part and components in the snowplow were created. The models were used for the virtual assembly to simulate the motion of the decelerators.

MATERIALS AND METHODS

Design of the drive scheme for the deceleration system

For a decelerator, it is crucial to design a speed-reducing and torque-increasing device. This device matches the rotational speed of the combustion engine to the speed of the output shaft, and gives solution to the connection between the engine with a high speed and low torque and the shaft with a low speed and high torque. Figure 1 shows the appearance of the snowplow decelerator for the agricultural greenhouse. Considering the small installation space of the decelerator as well as the large drive power and ratio, a reasonable selection of the driving type for the decelerator is a key step to design the snowplow. According to the mechanical drive theory, drive types can be used in snowplow such as the fixed axis gear, the harmonic gear, the NGW-type planetary gear, the N- and NN-type planetary gear with few teeth difference.

行了理论计算，采用改进的蚁群算法建立了寻优模型，给出寻优结果，并与传统优化设计方法进行比较。采用有限元分析对减速器关键部件进行校核，根据校核结果进一步优化结构设计。建立三维实体模型和虚拟装配，对减速器进行运动仿真研究。

材料与方法

减速系统传动方案设计

减速器设计的关键是能够设计使内燃机转速与输出轴转速相匹配的减速增矩装置，解决内燃机转速高、扭矩小，与输出轴转速低、扭矩大之间的连接。农业大棚清雪车外形如图 1 所示，由于减速器的安装空间小，需要传递的功率和传动比大，因此合理选择减速器传动类型是设计扫雪机械的关键步骤。从机械传动的理论来讲，扫雪机械可以采用定轴轮系、谐波齿轮传动、NGW 型行星轮系、N 型少齿差行星轮系及 NN 型少齿差行星轮系等传动方式。
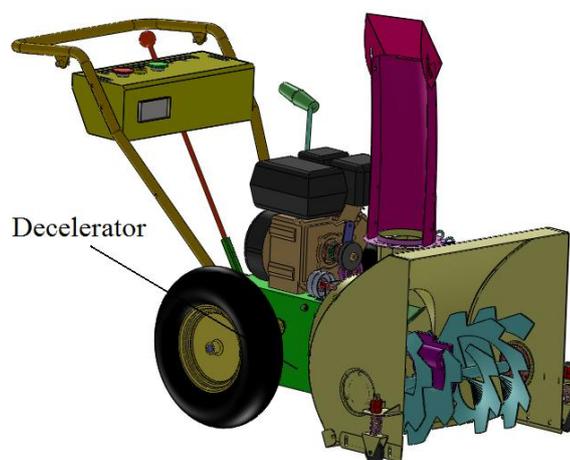

Fig.1 - Appearance figure of snowplow's decelerator for agricultural greenhouse

The fixed axis gear and the harmonic gear cannot meet the requirements for being constrained by the outer diameters. The NGW-type planetary gear, as shown in figure 2, has a drive ratio which is greater than 10. In such a structure, the power from the first-stage gear to the second-stage gear is the same as the input power. As the increasing of stages, the forces on post-stage gears become larger. And under the restriction of gear materials, this driving type is hard to meet the torque requirements [8].

由于其外径尺寸的限制，定轴轮系、谐波齿轮传动不能满足要求。NGW 型行星轮系传动比在 10 以上，结构简图如图 2 所示，由于该结构中第一级传递给第二级的功率与输入功率一样大，随着级数的增多，后一级所受的力逐渐增大，受齿轮材料的限制很难达到预定的扭矩要求[8]。

The driving of N-type planetary gear is as shown in figure 3. To get a large driving ratio, modified inside-engaged gears must be adopted for driving. However, the calculation and machining of such gears turn to be complex. Meanwhile, a larger modification coefficient of the gear pair corresponds to a larger angle of engagement, which will increase the radial force. Further, the output unit has strict requirements for the machining accuracy, and the working life will be shortened because of the high speed of bearings of the rotating arm.

The NN-type driving device consists of two pairs of inside-engaged gears by which the function of the deceleration and output can be achieved, and the gear shaft or internal gear is directly used as the output unit. Figure 4 shows its driving diagram. This type has a high driving ratio but low efficiency. And, when the rotating arm rotates at a high velocity, the noise caused by the rotation, is difficult to be completely eliminated even by balancing weight.

The closed epi-cyclic gear train is a combination of a 2-DOF differential gear mechanism and a 1-DOF stand planetary gear mechanism. Figure 5 shows its driving diagram. The input power can be split apart as a direct output-power after being transferred to the differential gears. Meanwhile, the differential gear mechanism can transfer its part power to the stand planetary gear mechanism. The transferred power is outputted together with the power of the differential mechanism. By considering small pipe diameters and splitting the power to make the gears of stage 2 to suffer a smaller torque, such a mechanism system is appropriate to the large torque output of a snowplow decelerator.

N 型行星轮系的传动比是靠一对内啮合齿轮的齿数差实现的，其传动简图如图 3 所示。该轮系要实现大的传动比必须采用变位的内啮合齿轮传动，这样轮系的计算、加工变得复杂了，同时齿轮采用较大的变位系数，传动啮合角也较大，使其径向力增大。另外，其输出机构对制造精度要求较高，转臂轴承的转速较高，使其使用寿命缩短。

NN 型传动装置由两对内啮合齿轮副组成，共同完成减速与输出任务，由齿轮轴或内齿轮直接输出，传动简图如图 4 所示。该类型传动的传动比较大，但是效率不高。且当转臂的角速度很大时，在其运转中会产生一定的噪声，即使采用平衡重量也难于完全消除。

封闭周转轮系是由一个二自由度的差动齿轮机构与一个单自由度的准行星齿轮机构封闭组合而成的，其传动简图如图 5 所示。输入功率传递给差动齿轮机构后可以进行分流，一方面直接输出功率，同时，差动齿轮机构又将部分功率传给单自由度的准行星齿轮机构，且经其变换后的输出功率与前者的输出功率一起进行输出。该机构在满足小尺寸管径的情况下，将功率分流，使得第二级齿轮机构承受较小的扭矩，适合扫雪机减速器的大扭矩输出要求。
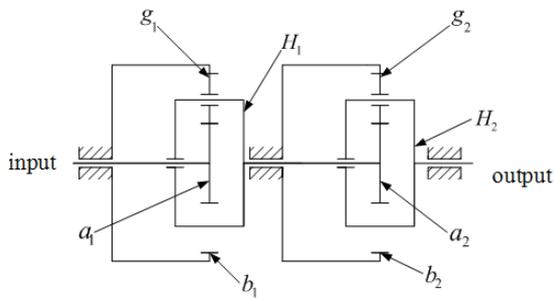

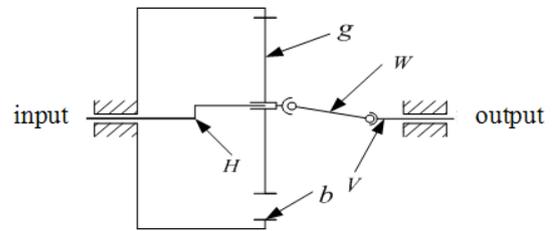**Fig.2** - Driving diagram of the NGW type planetary gear

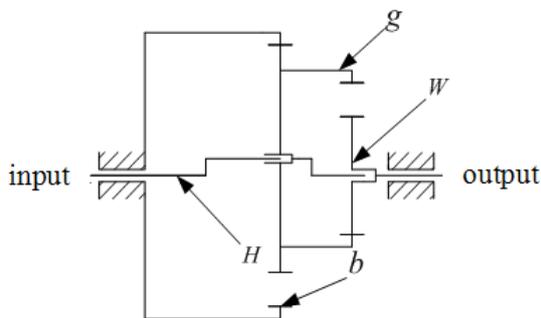**Fig.3** - Driving diagram of the N type planetary gear

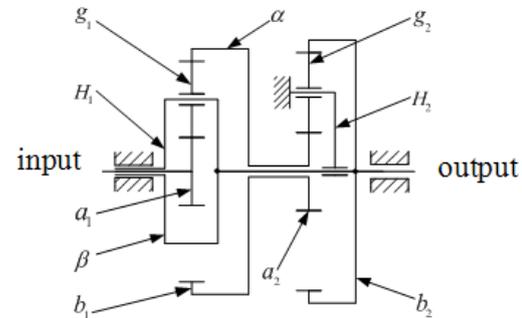**Fig.4** - Driving diagram of NN type planetary gear

Fig.5 - Driving diagram of closed epi-cyclic gear

The Ant Colony Algorithm only can be a solution to the unconstrained optimization and univariate problems. However, the snowplow design involves constraint conditions and multiple variations which are difficult to be solved by the Ant Colony Algorithm.

蚁群算法只能解决无约束优化问题和单变量问题，而扫雪机械设计问题中出现有约束条件和多变量问题，蚁群算法难以解决。

INMATEH·–·*Agricultural Engineering*

Here we apply a combination of the Ant Colony Algorithm and the Interior Point Penalty Function in the parameter optimization design of the snowplow. The multi-constraint optimization in formula (1) can be translated into the unconstrained optimization in formula (2) [2]:

这里我们将蚁群算法和内点惩罚函数法结合后应用在扫雪机减速器的参数优化设计中，将公式(1)的多约束优化问题转变为公式(2)的无约束优化问题[2]：

$$\begin{cases} \min f(x) \\ s.t. g_j(x) \le 0 (j = 1, 2, \cdots, m) \end{cases} \tag{1}$$

$$\phi(x, r) = f(x) - r \sum_{j=1}^{m} \frac{1}{g_j(x)} \tag{2}$$

Where r is a sequence of the penalty factors in a descending order, and goes to zero: $r^0 > r^1 > r^2 \cdots \to 0$. $\sum_{j=1}^{m} \frac{1}{g_j(x)}$ is called barrier function. Determine variables based on the design requirements, as shown in table 1, there are 8 variables.

其中 r 为惩罚因子，它是由大到小且趋近于 0 的数列，即 $r^0 > r^1 > r^2 \cdots \to 0$。$\sum_{j=1}^{m} \frac{1}{g_j(x)}$ 称之为障碍项。根据设计要求确定变量如表 1 所示，共有 8 个变量。

Table 1

Optimization design parameters variables of the decelerator

Parameters	Module (mm)	Teeth of Sun Gear	Teeth of Planet Gear	Tooth Width (mm)
Stage 1	m_1	z_1	z_2	b_1
Stage 2	m_2	z_1'	z_2'	b_2
Valid digit	3	2	2	2

To set the constraint conditions: pitch diameters of the internal gears in two stages should not exceed 117 mm, the driving ratio should be larger than 10, the contact ratio of all gears should be larger than 1.2, the contact fatigue strength and the teeth bending strength should be less than the allowable value.

The minimum pitch volume of the decelerator's gears is regarded as the optimization objective. Firstly, the constraint objective function can be built as follows:

建立约束条件，两级内齿轮分度圆直径均不能超过 117mm，传动比大于 10，所有齿轮重合度均大于 1.2，啮合接触疲劳强度和齿根弯曲强度小于许用值。

以减速器齿轮分度圆体积最小为优化目标，首先建立有约束目标函数为：

$$V = \pi[m_1^2 b_1(z_1^2 + 4z_2^2) + m_2^2 b_2(z_1'^2 + 3z_2'^2)] / 4 \tag{3}$$

The objective function can be translated into the unconstrained optimization by adopting the Interior Point Penalty Function:

采用内点惩罚函数法将目标函数转化为无约束优化问题：

$$\phi = V - r \sum_{j=1}^{13} \frac{1}{g_j(x)} \tag{4}$$

After being optimized by the Ant Colony Algorithm and the Interior Point Penalty Function, the results are shown in table 2:

通过蚁群算法和内点惩罚函数法优化后的结果如表 2 所示：

Table 2

Results of the decelerator parameter optimization

Parameters	Module (mm)	Teeth of Sun Gear	Teeth of Planet Gear	Tooth Width (mm)
Stage 1	$m_1 = 2.5$	$z_1 = 16$	$z_2 = 14$	$b_1 = 59$
Stage 2	$m_2 = 2.0$	$z_1' = 21$	$z_2' = 15$	$b_2 = 62$

Meanwhile, the optimum values of the driving ratio, the output speed of the differential internal gears, the rotational speed of the planet gear, the torque of the output shaft, and the driving efficiency can be obtained. On account of the practical work conditions of the deceleration system, different FEA methods were adopted for different key components.

Due to the complexness of the model, we built a 3D model using Pro/E and then imported it into the software of ANSYS in the format of IGES. The model can be meshed, constrained with boundary conditions, loaded and treated by other finite element operations in ANSYS.

Finite element stress analysis of the bearing prong of stand planet mechanism

In the deceleration system, 33% power was split for stage 1, and the left 67% for stage 2. The stand planet mechanism has to suffer more stresses, thus, FEA for its bearing prong should be carried out.

As shown in figure 6, the point O is the centre of the planet bracket and the point O is the centre of the bearing bore. Given that the torque on the planet bracket is T, the number of the pinion gears is 3, the bearing prong has been fixed on the body frame; and the torque on each bearing bore is one-third of that of the bracket, namely T/3. A rough calculation may be made when the requirements do not need to be strictly satisfied. In this paper, a calculation based on the distribution function was proposed, and the pressure distribution on bracket was assumed to follow the cosine function, with the peak value A and unit MPa. Then, p, the pressure distribution function, can be obtained as follows:

同时可以获得传动比、差动机构内齿轮输出转速、行星机构行星轮转速、输出轴上的扭矩、传动效率的最佳值。结合减速系统工作的实际情况,不同的关键部件采用不同的有限元分析方法。

由于模型比较复杂,所以模型在 Pro/E 中建立,然后将三维模型以 IGES 的格式导入 ANSYS 中。在 ANSYS 中进行网格划分、定义边界条件、施加载荷等有限元操作。

准行星机构轴承支架有限元应力分析

在减速系统中,功率分配为第一级 33%,第二级 67%。准行星机构受力较大,故对准行星机构轴承支架有限元分析。

如图 6 所示,O 为行星架中心,O' 为轴承孔中心。已知作用在行星架上的扭矩为 T,小齿轮个数为 3,该轴承支架固定在机架上,作用在每个轴承孔上的扭矩为行星架上扭矩的 $T/3$,通常在要求不高的情况下,我们可以采用粗略估算法,本文提供一种基于分布函数的计算方法。规定作用在行架上的压力以余弦函数分布,设该压力峰值为 A,单位为 MPa,压力分布函数 p 为:

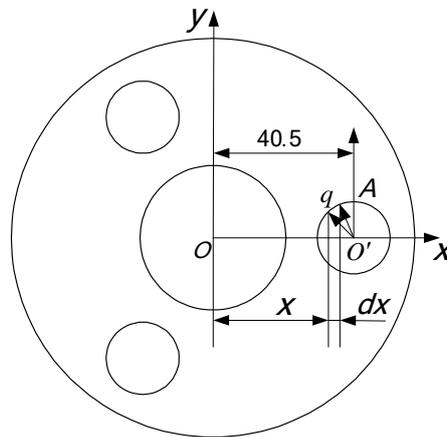$$p = A\cos\frac{(x-40.5)}{21}\pi \tag{5}$$

Fig.6 - The stress map of the bearing prong

As shown in figure 6, the distance from the point O, the centre of the planet bracket, to the point O', the centre of the bearing bore, is 40.5 mm. x (varying from 30 to 51 mm) is the horizontal line distance between any point on the circle and the bearing prong centre O. $\theta = \angle$ qO'A, θ varying from 0 to π, is the angle between the pressure q and y-axis. dy is a differential variable with the direction along the moment arm, and the differential area can be calculated by:

如图 6 所示,其中轴承架中心 O 到轴承孔中心 O' 的距离为 40.5 mm,x 为圆周上任意点与轴承架中心 O 的水平直线距离,在 30-51 mm 之间变化。θ 是压力与 y 轴的夹角,即 $\angle$qO'A,在 0-π 间变化。沿力臂方向取一微变量 dy,微面积为:

$$dS = 9dx \tag{6}$$

17

Where the depth of the bearing bore is 9 mm. The differential force on this area and perpendicular to y-axis is formula (7), And the differential torque is $dT = xdF$. Appling Eq. (7), we get formula (8).

其中轴承孔深度为 9 mm。作用在此面上的垂直于 y 轴方向的微力为公式（7），则微扭矩为 $dT = xdF$，将公式 (7)代入得公式（8）。

$$dF = pdS = 9Adx\sin\theta\cos[(x-40.5)\pi/21] \tag{7}$$

$$dT = 9Ax\sin\theta dxd\theta\cos[(x-40.5)\pi/21] \tag{8}$$

Then, the torque of the whole area is:

则作用在整个面上的扭矩为：

$$T = \int_0^\pi \int_{51}^{30} 9Ax\sin\theta\cos\frac{(x-40.5)}{21}\pi dxd\theta \tag{9}$$

We can get the solution A by substituting T into Eq. (9). Firstly, we set a local coordinate system with the origin at the centre of the bearing bore, and define load function according to this coordinate. In ANSYS, the fixed bolt holes on the bearing prong have been fully constrained. And the pressure p distributes on the upper surfaces of these three bearing bores (i.e. the upper surface of the circle O' in figure 6). By applying the load function, a static solution can be obtained. Figure 7 show the mesh and the stress, respectively.
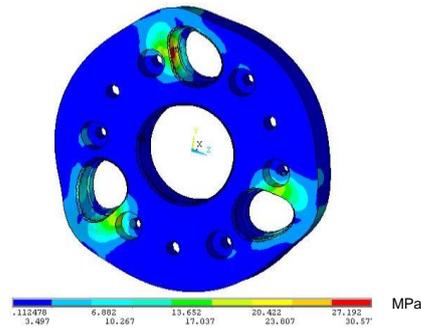
将 T 代入公式(9)，解得 A 。首先在轴承孔中心建立局部坐标系，以此坐标系为参照定义载荷函数。在 ANSYS 中将轴承支架在固定螺栓孔处全约束，将压力 p 分布在三个轴承孔的上表面(即图 6 中圆 O' 的上表面)，通过载荷函数加载，进行静力求解。其网格图与应力云图如图 7 所示。

| (a) The mesh map | (b) The stress map |

Fig.7 - FEA of the bearing prong

From the stress nephogram, it can be found that the maximum stress, which is less than the allowable value of the bearing prong material, was generated at the bearing bore farthest from x-axis. With the satisfaction of installation and strength conditions, we can minimize the size by adjusting the width of the bearing prong, and thus to reduce the weight of the whole deceleration system.

由应力云图可知最大应力的产生位置在轴承孔上到 x 轴最远处，其值小于轴承架材料的许用值，轴承架安全。通过调整轴承架的宽度，在满足轴承安装条件和强度要求的情况下使其体积最小，减轻减速系统整机重量。

FEA of the connecting joint

One end of the joint was fixed to the internal gear ring of the differential mechanism, and the other was connected with the larger gear of the stand planet mechanism. According to the calculation, the torque on the internal gear ring of the differential mechanism is T, the joint was fixed to the internal gear ring of the differential mechanism by four bolts. The number of involute spline teeth: $z = 8$, with pressure angle of 30°. The working line of the spline L=40 mm. Assume that the involute spline works under ideal conditions, and all eight gears are surface-contacted. Estimating the area of the contact surface of each gear to be S, and the working radius of involute spline to be R, and assuming the unit surface pressure to be p, then one can obtain the following expression: $T = z \cdot p \cdot S \cdot R$, by substituting T,

联接接头有限元应力分析

联接接头一端固定在差动机构内齿圈上，另一端和准行星机构大齿轮联接。根据计算出作用在差动机构内齿圈的扭矩为 T，联接接头采用 4 条螺栓固定在差动机构的内齿圈上，渐开线花键齿数 z =8，压力角为 30 度，渐开线花键工作长度为 L=40 mm，假设渐开线花键工作在理想状态，8 个齿全部面接触。粗略估算每个齿的接触面积为 S，渐开线花键工作半径为 R，则设作用的单位面压力为 p，可得：$T = z \cdot p \cdot S \cdot R$，将 T 、 z 、 S 、 R 代入公式，求得单位面压力 p。在 ANSYS 中，将联接接头用于

z, S and R into Eq., one can get the solution of the unit surface pressure p.

The eight working surfaces of the involute spline were picked to apply the surface pressure, respectively, as shown in fig.8-(a). The stress map is shown in fig.8-(b).

固定在差动机构的内齿圈的四个盲孔完全约束。
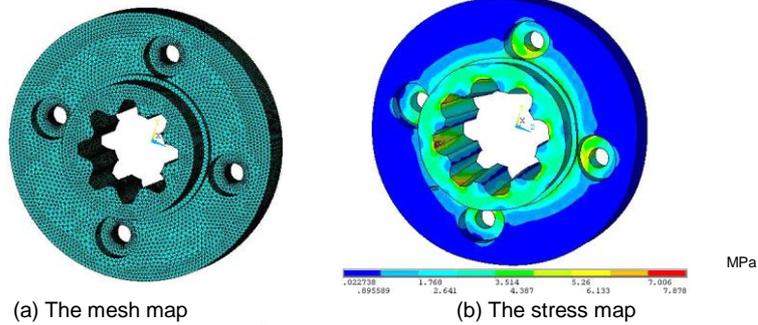
分别选择渐开线花键的 8 个工作面，施加面压力，如图 8-(a)所示，应力图如图 8-(b)所示。

(a) The mesh map	(b) The stress map

Fig.8 - FEA of the joint

FEA of the fixed bracket

The fixed bracket was used for fixing the bearing prong and the sleeve of the stand planet mechanism. The bracket at one end of the differential mechanism was subject to no moment and constraint conditions, so this part was cut off for improving the calculation speed. Only the constrained and torqued part was left for analysis. The fixed bracket and the bearing prong of the stand planet mechanism were connected by 6 bolts. The influence of the thread was neglected. According to the calculation, the torque on the bearing prong of the stand planet mechanism is T, the torque on each bolt hole is T/3, and the working area is S. It is assumed that each surface works under the ideal conditions and all 6 holes are surface-connected. The working radius of the torque is R=40.5 mm and the unit surface pressure is p, then: $T/3 = 6p \cdot S \cdot R$ .The value of p can be determined by putting *T*, *S* and *R* into Eq.

In ANSYS, the outside ring of the fixed bracket was fully constrained. The eight working surfaces of the bolt holes were picked to apply the surface pressure, respectively. The elasticity modulus is 2.1×105 MPa. The Poisson's ratio is 0.3.

The automatic mesh generation was used by assigning 4 mm to the overall size of the mesh. Next, elements at bolt holes were refined with a mesh size of 2 mm, as shown in figure 9-(a). The stress diagram is shown in figure 9-(b).

固定支架有限元应力分析

固定支架用于固定准行星机构轴承架和套筒。由于在差动机构一端的支架不受力矩作用，也没有约束存在，所以为了提高有限元计算速度将其切下，只留下受约束和受扭矩的部分进行分析。固定支架和准行星机构的轴承架用 6 条螺栓连接，忽略支架上的螺纹等次要因素，根据计算出作用在准行星机构轴承支架上的扭矩为 T ，则每个螺栓孔所受的扭矩为 $T/3$ ，工作面积为 S 。假设各个面工作在理想状态，6 个孔全部面接触。扭矩工作半径为 R=40.5mm ，设作用的单位面压力为 p ，可得：$T/3 = 6p \cdot S \cdot R$ ，将 T 、 S 、 R 代入公式可得 p 。

在 ANSYS 中，将固定支架外圈完全约束，分别选择螺纹孔的 6 个工作面，施加面压力。在材料属性中指定弹性模量为 2.1×10^5 MPa ，泊松比为 0.3。

指定网格的总体尺寸为 4 mm ，自动划分网格，然后将螺纹孔处单元选择进行细化，网格总体尺寸为 2 mm ，如图 9-(a)所示，应力图如图 9-(b)所示。

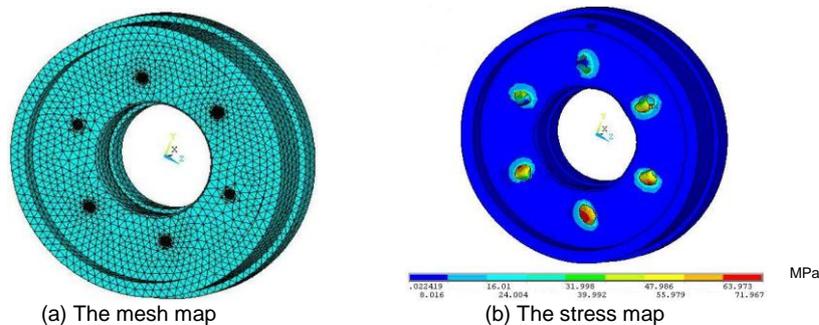| (a) The mesh map	(b) The stress map

Fig.9- FEA of the fixed bracket

From the analytic results, it can be found that the maximum stress was generated at the bolt holes. Because the bearing prong of the stand planet mechanism has a larger torque, the stress of a single hole can be reduced by appropriately increasing the number of holes.

Dynamic FEA of the gear meshing process

In the gear meshing process, the stress distribution of a gear is varying as the motion of the contact-point. According to the classical gear theories, the approximate load distribution was used instead of the concentrated-forces on the pitch circle, so some errors may be generated in the calculation results. While in the FEA, the practical process of the gear meshing can be effectively simulated. The changes of the stress at different positions of the gear can be observed. Besides, the classical gear theories regard the gear as being rigid, without considering that the gear deformation will generate impacts on both contact-forces and the contact ratio of a gear pair. On the contrary, the FEA takes the elasticity into account. The simulation of the meshing process of a gear pair can be realized by using the LS-DYNA. A thorough understanding about the distributions of bending stresses and contact stresses can be achieved.

After inputting the IGES profile generated by Pro/E into ANSYS, some simple treatments were made. And then the FEA was carried out. In this analysis, the surface-to-surface contact was used. The 3D solid element named Solid 164 which supports the LS-DYNA analysis was used. In order to improve the computational accuracy, the mesh of the contacting area was refined. Meanwhile, for the purpose of saving computer resource and speeding up the analysis, rough meshes were applied in other areas of the gear which were not engaged in the contact. Figure 10 shows the mesh results.
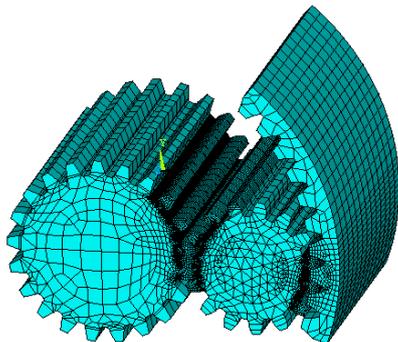
从分析结果我们可以看出，应力最大处在螺栓孔处。由于准行星机构的轴承支架上所受扭矩较大，所以可以通过适当增加螺栓孔的个数来降低单个螺栓孔的应力。

齿轮啮合过程动态有限元分析

齿轮在啮合过程中，其应力分布是沿接触点变化的，经典的齿轮设计理论是将分布载荷近似成集中力作用在分度圆上，计算出的结果有一定误差。用有限元法计算可以更有效地仿真齿轮啮合的实际过程，并且能观察出轮齿上各处应力的变化情况。经典的齿轮分析方法将齿轮假设为刚体，没有考虑齿轮变形对齿面接触力和齿轮副重合度的影响。而有限元将齿轮做弹性件处理，采用 LS-DYNA 有限元分析软件，对齿轮啮合过程进行有限元仿真分析，对其弯曲应力和接触应力分布状况进行透彻了解。

将 Pro/E 中生成的 IGES 文件导入 ANSYS 中进行简单的处理以便进行有限元分析。本文选择面与面接触，选用三维实体单元 Solid164 划分网格，该单元支持三维实体模型的 LS-DYNA 有限元分析。为了提高计算精度，在进行网格划分时，对于参于接触的轮齿部分进行了网格细化。而为了节约计算机资源，提高分析速度，将不参于啮合的其它轮齿采用粗略的网格进行单元划分。网格如图 10 所示。

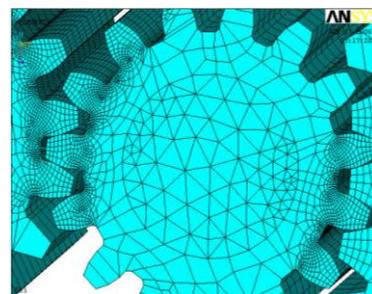**Fig.10**- Mesh of the FEA in the gear mesh simulation

During the meshing process, a follow-load should be exerted because of the rotation of the gears. In ANSYS, the 3D solid shell element named Shell 163 can be easily exerted with the surface load. By such an advantage, we may use Shell 163 to create several auxiliary planes which are similar to spokes. The surface pressures were applied on these planes which are always contacted with these "spokes". Hence, a constant resultant torque can be obtained to realize the exerting of the load during the meshing process of the gear pair. After the finite element computation by LS-DYNA, a module of ANSYS, the contact stress distribution of a certain moment is shown

由于齿轮在啮合分析过程中转动，所以需要施加跟随载荷。在 ANSYS 中的 Shell163 三维实体壳单元可以很方便地施加面载荷。利用 Shell163 单元创建若个类似于轮辐的辅助平面，对其施加面压力。其大小和方向始终作用于轮辐上，合成为一个恒定的扭矩，实现了在齿轮副啮合过程中施加外载荷，通过利用 ANSYS LS-DYNA 模块经过有限元的求解后，在某一个瞬时的接触应力的分布情况如图 11

in figure 11. It can be seen that the distribution of the contact stress in figure 11 matches entirely with the classical Hertz theory. It also testifies the precision and accuracy of the finite element model developed in this paper.

Figure 12 shows the contact stress distribution of a single tooth surface of a certain moment. It can be known from the equivalent stress map that the contact stress distribution of the tooth surface is in linear with slightly larger values near the sides of the tooth. In general, the stress shows a uniform distribution. The analytical results of the stress show that the gears designed in this paper are able to meet the requirements of contact strength. Besides, the meshing between two neighboring gears reveals that the contact ratio of a gear pair is larger than 1.2.
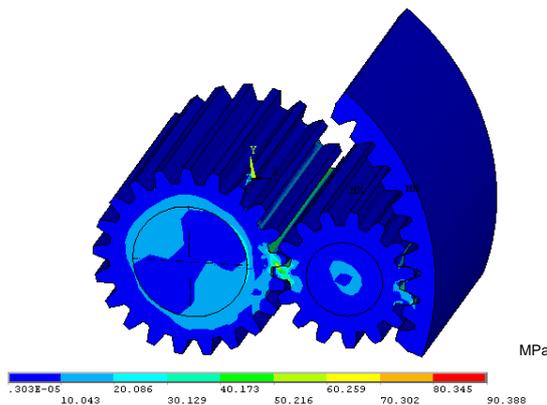
所示。由图可以看出其接触应力的分布与经典的赫兹理论是完全相符的，从而也验证了本文提出的有限元模型的精度与正确性。

单个齿面上某一瞬时的接触应力的分布情况如图 12 所示。通过该图等效应力可以看出，齿面上的接触应力成线性分布，两侧略大，从总体上看，应力分布比较均匀。分析出的应力结果表明，本文设计的齿轮满足接触强度要求。另外，通过相邻两个齿进入啮合的情况可以看出，齿轮副的重合度大于 1.2。
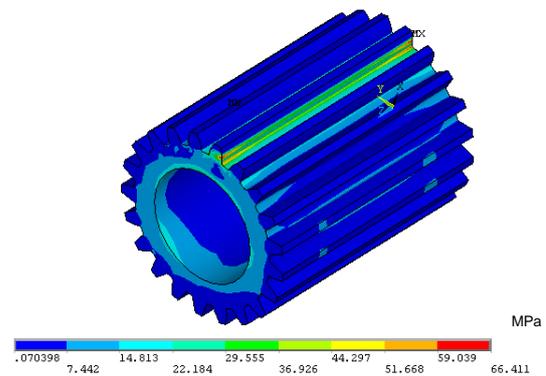

Fig.11- The Contact stress of gear pair

Fig.12- The Contact stress of the larger gear

Motion simulation on the operation of the decelerator

Simulation on the motion of the deceleration system was performed. The interference detection and modification were done based on the simulation results. The 3D components and 3D assembly of the efficient oil-injecting pipe in the deceleration system were developed. The reasonability of this design was proved by comparing the simulation results with the theoretical values.

Modeling of differential mechanism and the stand planet mechanism

Considering their small pitch diameters, the sun gear and the planet gear were designed to be of the "shaft shape" with short teeth to enhance the strength. For the convenience of assembly, the planet bracket, with two plates on the right and left sides, was designed. That is one trochal disk on each side and fixed by bolts. The differential mechanism, with function of power-splitting, directly outputs a part of the power to the output-shaft through the planet bracket. Another part of the power is output through the stand planet mechanism. Taking the uniform load of the planet gear into account, the involute spline connection was adopted between the right planet bracket and the output-shaft, as well as between the internal gear ring and the sun gear of stage 2. The exploded and assembly drawing of the differential mechanism are shown in figure 13-(a) and (b), respectively.

减速器工作状况运动仿真

对减速系统进行运动仿真并进行干涉检测，根据仿真结果对高效采油管内减速系统的三维零件和三维装配进行修改，将仿真结果和理论值进行比较，验证了该方案的合理性。

差动机构和准行星机构建模

考虑到太阳轮和行星轮的分度圆直径较小，为增加齿轮的强度，将太阳轮和行星轮设计成齿轮轴及短齿齿形；考虑到装配方便，将行星架设计成左右侧板型，即在左右各有一个轮盘，中间用螺栓固定。由于功率分流，所以差动机构将一部分功率通过行星架直接输出到输出轴上，另一部分通过准行星机构输出，考虑到行星齿轮的均载问题，将右侧行星架和输出轴采用渐开线花键联接，内齿圈和第二级太阳轮也采用渐开线花键联接。差动机构模型爆炸图如图 13-(a)所示，装配图如 13-(b)图所示。
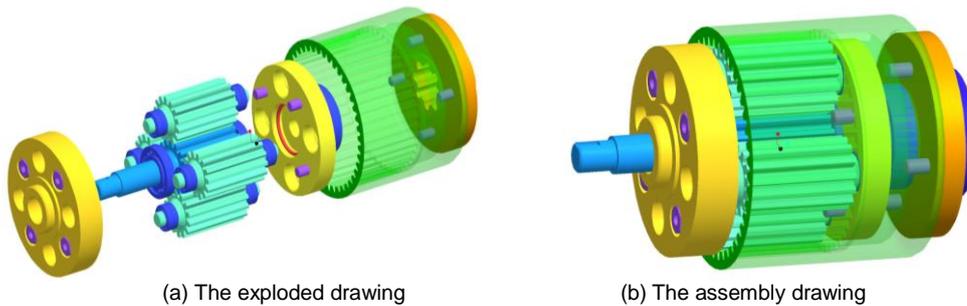
(a) The exploded drawing   (b) The assembly drawing

Fig.13- Exploded and assembly drawing of the differential mechanism

Like the design of the differential mechanism, the exploded drawing of the stand planet mechanism is shown in figure 14-(a) and the assembly drawing is shown in figure 14-(b).

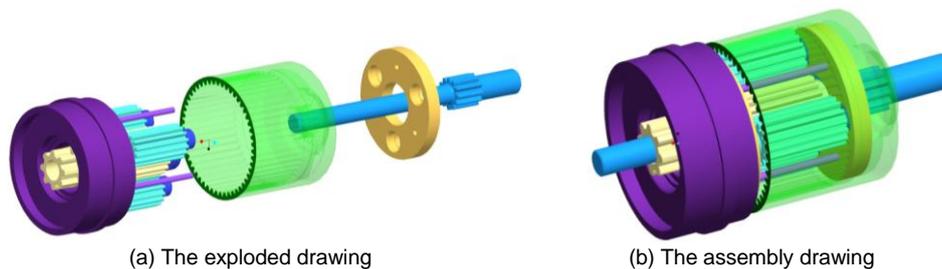同差动机构设计一样，准行星机构模型爆炸图如图 14-(a)所示，装配图如图 14-(b)所示。

(a) The exploded drawing   (b) The assembly drawing

Fig.14 - Exploded and assembly drawing of the stand planet mechanism

End-caps and outer-sleeves were designed and installed on both sides of the decelerator for assembling the differential mechanism, the bracket and the stand planet mechanism. Under the assembly mode, the position and volume of the interference were figured out through detections. The structure adjustment or the assembly readjustment was made until they met the requirements of interference detection. In this study, the global interference of the decelerator was detected, and the adjustment was made based on the detection results.

RESULTS
Motion analysis of the decelerator
Figure 15 shows the speed curve of the stage-1 differential mechanism. It can be seen from the map that, when t=10 s, the speed of the input shaft is 100 deg/s, the internal gear ring is -23.19 deg/s (the minus here means its angular velocity is opposite to the speed of the input shaft), and the planet bracket is 9.59 deg/s. Likewise, the acceleration curve and its value can also be obtained.

Speed and acceleration curves of the planet mechanism components are similar to that of the differential mechanism. Calculated by the theoretical driving ratio, the theoretical calculation values match to the results of simulation when the motor input q=10t. Preferable simulation results were obtained. The validity of the system was verified. A special mechanical seal for the input and output shaft is designed. It can atenuate the abrasion automatically when the material used is destroyed.

在减速器两端设计了端盖以及外套筒，将差动机构、支架、准行星机构等约束装配。在装配模式下，通过干涉检测，计算出干涉的位置和干涉的体积，根据计算的结果进行结构调整或者重新调整装配，直到通过干涉检测为止，本设计对减速器全局干涉进行了检测并根据结果进行了调整。

结果
减速器运动分析

第一级差动机构速度曲线如图 15 所示，由图可以看出，当 t=10s 时，输入轴速度为 100 deg/s ；内齿圈为-23.29 deg/s ，负号表示其角速度与输入轴相反；行星架为 9.59 deg/s ，加速度曲线和加速度值同样可以得到。

准行星机构各元件速度和加速度曲线和数值与差动机构类似。按理论计算的传动比计算，当电机输入为 q=10t 时，其理论计算值与仿真结果相吻合，得到了较好的仿真结果，证明了系统的正确性。设计可补偿式机械密封，保证了减速系统的安全。
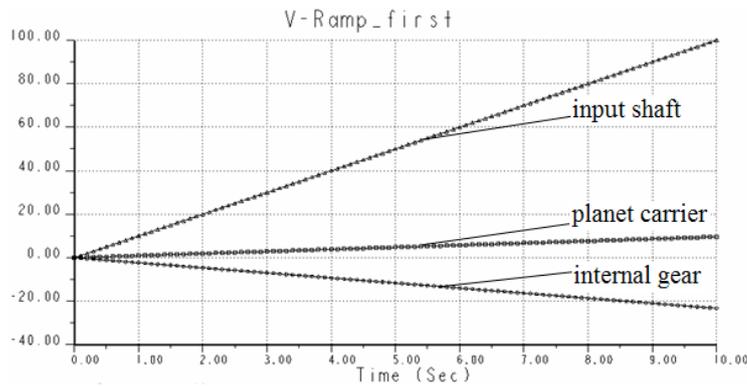
Fig.15- The V output map of the differential mechanism when q=10t

Prototype test for an agricultural greenhouse

The main parameters of the new type decelerator are superior to the traditional decelerator through comparison as shown in table 3.The new decelerator was applied in the snowplow for an agricultural greenhouse. The technical parameters of new snowplow are as follows: The maximum working load is 2200 lbs/min. The maximum throwing distance is 10-15m. The maximum working width is 28". The maximum working thickness is 22". The chute rotating angle is 190 degree. The power distribution of the snowplow was smooth. The snowplow had a stable body and a low failure rate. It played a good performance in snow removing, as shown in figure 16.

样机测试

将新型减速器与传统减速器对比，如表 3 所示，新型减速器的主要参数优于传统减速器。将新型减速器在大棚清雪车上进行测试，技术参数如下：最大工作载荷 2200 lbs/min，积雪最大抛投距离 10-15 米，最大工作宽度 28"，最大清雪厚度 22"，抛雪筒旋转角度 190 度。大棚清雪车动力分配平稳，车体稳定，故障率低，新型减速器工作状态良好，如图 16 所示。

Table 3

Parameters contrast between traditional decelerator and new type decelerator

Decelerator	Transmission Mode	Power Allocation	Power Range(KW)	Maximum Deceleration	Diameter (mm)	Transmission Efficiency	Maximum Torque (mm)
Old type	Fixed axis gear Train	Power reflux	7.35-16.75	6	190×180	94%	610
New type	Closed epi-cyclic gear train	Power Split	7.35-21.54	10.43	ϕ 138	96.48%	750.35

Fig.16- Snowplow equipped with the new decelerator for a greenhouse

CONCLUSIONS

(1) By considering the working conditions of the decelerator, several driving types of internal gearing planetary gears with the coaxial deceleration were compared. The closed epi-cyclic gear matches the rotational speed of the combustion engine to the speed of the output shaft, and gives solution to the connection between the engine with a high speed and low torque and the shaft with a low speed and high torque.

(2) By combining the Ant Colony Algorithm and the Interior Point Penalty Function, a step optimizing model

结论

（1）通过分析减速器工作环境，将能实现同轴减速的几种内啮合行星齿轮传动进行分析比较，最终采用具有功率分流功能的封闭周转轮系。该轮系是能够使内燃机转速与输出轴转速相匹配的减速增矩装置，解决内燃机转速高、扭矩小，与输出轴转速低、扭矩大之间的连接。

（2）将基本蚁群算法和内点惩罚函数法结合起来，提

was proposed to cope with the problems on multivariable, multiple constraints and multiple discrete points. It overcomes the difficulties in mechanical optimization design by only using the Ant Colony Algorithm.

(3) The contact element in ANSYS was adopted to the FEA of the gearing in the stand planet mechanism suffering a larger load. In addition, a new loading method was presented to exert the dynamic forces of the gears. This method can reflect the real stress-changes of the gear meshing process. Motion simulation of the whole decelerator system was carried out. The decelerator was restructured according to the FEA results, for achieving the optimum state.

REFERENCES

[1]. Liguang Chen, Songlin Wang, Jiefu Wang (2012) - *Mechanism analysis of snow-ice removing using vibration and optimization of vibration roller,* Construction Machinery, vol. 22, no.2, pp.102-108;

[2]. Jin Xiangyang, Zhao Lili, Sun Zhihui (2013) - *Optimal design of snow collector of a shed snow remover based on genetic algorithm.* International Journal of Applied Mathematics and Statistics, vol.51,no.24, pp.393-400;

[3]. Maruyama Toshisuke, Takimoto Hiroshi, Ogura Akira, et al. (2015) - *Analysis of snowpack accumulation and the melting process of wet snow using a heat balance approach that emphasizes the role of underground heat flux,* Journal of Hydrology, vol.522, no.3, pp.369-381;

[4]. Solovey Aleksey (2013) - *Feasibility of using an absorptive cover for ice, snow or water removal from random surface,* Progress in Electromagnetic Research Symposium, vol.25, no.3, pp.149-154;

[5]. Sugiyama Hirosi, Kinoshita Masao. (1982) – *Experimental studies on fracture of compacted snow,* Quarterly Report of RTRI, vol.23, no.3, pp.124-128;

[6]. Wå&ring, hlin Johan, Leisinger Sabine et al. (2014) - *The effect of sodium chloride solution on the hardness of compacted snow,* Cold Regions Science and Technology, vol.102, no.6, pp.1-7;

[7]. Whlin Johan, Klein-Paste Alex (2015) -*The effect of common de-icing chemicals on the hardness of compacted snow,* Cold Regions Science and Technology , vol.109, no.1, pp.28-32;

[8]. Xinyu Wei,Yaqin Li,Junfa Wang.(2013) - *Modeling and Kinematics Simulation of Concave Disk Mechanism for Icebreaking ＆ Snow Removal Based on CATIA and ADAMS,* Journal of Agricultural Mechanization Research, vol. 34, no.1, pp.22-25;

[9]. Zhihui Sun,Youzhi Zhang,Xiangyang Jin.(2013) - *Optimization of structure parameters and analysis of dynamic characteristics of snow － collection spiral blade,* Journal of Harbin University of Commerce, vol. 29, no. 3, pp.303-308.

出"阶梯"寻优模型，解决基本蚁群算法在机械优化设计中遇到的多变量、多约束、多离散点等难点。

（3）采用有限元中接触单元对受力较大的准行星机构进行齿轮啮合接触有限元分析，使用新的载荷加载方法实现齿轮动态作用力，真实反映齿轮在啮合过程中的应力变化情况。对整个减速器系统进行运动仿真，根据分析结果对减速器结构进行调整，以达到最优。

参考文献

[1]. 陈礼光，王松林，王杰夫. (2012) -*振动清除冰雪机理分析及振动碾压碳优化*,建筑机械，第 22 卷，第 2 期,102-108;

[2]. 金向阳,赵丽丽,孙智慧.(2013) – *基于遗传算法的大棚清雪车集雪器的优化设计*,应用数学与统计，第 51 卷，第 24 期,393-400;

[3]. Maruyama Toshisuke,Takimoto Hiroshi,Ogura Akira, et al. (2015) -*基于地下热流的作用的热平衡方法对积雪堆积与融化的分析*,水文学,第 522 卷,第 3 期, 369-381;

[4]. Solovey Aleksey.(2013) –*利用雷达天线罩表面吸热层去除冰雪水可行性分析*,电磁研究进展研讨，第 25 卷,第 3 期,149-154;

[5]. Sugiyama Hirosi，Kinoshita Masao.(1982) - *压实雪的脆断性研究*, RTRI 季度报告, 第 23 卷, 第 3 期,124-128;

[6]. Wå&ring,hlin Johan, Leisinger Sabine,等.(2014)- *氯化钠溶液对压实硬雪硬度的影响*, 寒冷地区科学技术,第 102 卷, 第 6 期, 1-7;

[7]. Whlin Johan, Klein-Paste Alex.(2015) – *化学除冰对压实硬雪硬度的影响*,寒冷地区科学技术, 第 109 卷, 第 1 期, 28-32;

[8]. 魏鑫宇,李亚芹,王俊发. (2013) -*基于 CATIA 和 ADAMS 凹盘破冰除雪机构建模与运动仿真,* 农机化研究, 第 34 卷, 第 1 期,22-25;

[9]. 孙智慧,张友志,金向阳. (2013)-*集雪器螺旋叶片的结构参数优化及动力特性,* 哈尔滨商业大学学报, 第 29 卷, 第 3 期, 303-308.